ECCOMAS Congress 2016
VII European Congress on Computational Methods in Applied Sciences and Engineering
M. Papadrakakis, V. Papadopoulos, G. Stefanou, V. Plevris (eds.)
Crete Island, Greece, 5–10 June 2016

SENSITIVITY ANALYSIS OF HYDRAULIC FRACTURING USING AN EXTENDED FINITE ELEMENT METHOD FOR THE PKN MODEL

Hasini Garikapati[1], **Clemens V. Verhoosel**[1], **E. Harald van Brummelen**[1], **Pedro Diez** [2]

[1]Multi-scale Engineering Fluid Dynamics
Eindhoven University of Technology,Eindhoven, The Netherlands
e-mail: {h.garikapati, c.v.verhoosel, e.h.v.brummelen}@tue.nl

[2] Laboratori de Calcul Numric
Universitat Politecnica de Catalunya, Barcelona, Spain
e-mail: pedro.diez@upc.edu

Keywords: Hydraulic fracturing, PKN model, Extended finite element method, Sensitivity analysis, Uncertainty quantification

Abstract. *Hydraulic fracturing is a process that is surrounded by uncertainty, as available data on* e.g. *rock formations is scant and available models are still rudimentary. In this contribution sensitivity analysis is carried out as first step in studying the uncertainties in the model. This is done to assess which of the parameters are key drivers to the model's results. As a baseline model for hydraulic fracturing, the classical PKN model of hydraulic fracturing by Perkins and Kern (J. Pet. Tech. Trans. AIME, 222:937949 (1961)) and Nordgren (J. Pet. Tech. 253:306314 (1972)) which is widely used in the Oil and Gas industry to assist in the design of the hydraulic fracturing treatment is considered. The problem under consideration is characterized by a moving boundary, strong non-linearities and a singularity at the moving tip due to vanishing of the fracture aperture. Sufficient accuracy for such problems is required to obtain a high quality parametric sensitivity analysis and uncertainty quantification. In order to achieve this, various advanced numerical methods are studied. An XFEM approach is adopted to simulate the fracture initiation, propagation and opening of the fracture profile. Using this method, the sensitivity analysis of parameters such as fracturing fluid viscosity, fracture geometry characteristics, soil or rock formations properties via plain strain modulus and leak off coefficient (of the soil) are presented. The impact of these input parameters with respect to the output parameters such as the fracture length and width are discussed.*

1 INTRODUCTION

Hydraulic fracturing is the process of fracturing rock formations by a pressurized liquid to release hydrocarbon resources. This technique is essential for accessing vast new unconventional natural hydrocarbon reserves, which are otherwise inaccessible. Hydraulic fracturing processes are surrounded by uncertainty, as available data on *e.g.* rock formations is limited. The development of models and simulation tools to quantify the risks associated with hydraulic fracturing processes is indispensable. In this contribution, we study the influence of various sources of uncertainty on the hydraulic fracturing process, including characteristics of the fracturing fluid, rock properties, and leakoff parameters. The parameteric sensitivity analysis presented herein is an important first step in the development of an uncertainty quantification framework for hydraulic fracturing.

In order to perform a sensitivity analysis, it is preferable to use a deterministic model which is capable of mimicking the essential aspects of the process, yet remains sufficiently simple to allow for efficient numerical evaluation. In general, the ability to quickly evaluate the deterministic model is critical for many stochastic methods (*e.g.* Monte-Carlo simulations). Herein we consider the PKN model (Perkins-Kern-Nordgren) [1], [4] for hydraulically-stimulated vertical fractures, which computes the fracture aperture and length – two key quantities of interest in hydraulic fracturing– for a fixed fracture height (Figure 1). The PKN model is applicable when the vertical hydraulic fracture is bound within a horizontal permeable layer, and when its length is much larger than the height [2].

Although studied extensively, consideration of the PKN model in an uncertainty quantification framework remains an open research challenge. Attaining sufficiently accurate numerical results to perform a reliable sensitivity analysis (or, more generally, uncertainty quantification) is challenging due to the nature of the problem, which involves strong non-linearities and a moving boundary that degenerates at the tip [3]. The prevailing numerical techniques for the PKN model, which are based on explicit finite difference formulations [6], do not meet the accuracy requirements at acceptable computational costs. For this reason we employ the eXtended Finite Element Method (XFEM) to discretize the model. This numerical technique enables us to conduct a quantitative sensitivity study of the impact of various sources of uncertainty in hydraulic fracturing process.

This paper is organized as follows. In Section 2 we present the governing equations for the PKN model. In Section 3 we describe the XFEM discretization. The sensitivity analysis performed using the PKN model is presented in Section 4, where the effect of the various input parameters on the output of the process is studied. Finally, in Section 5 we draw conclusions and discuss future research directions.

2 FORMULATION

The problem setup for the PKN model [4] considered herein is schematically shown in Figure 1, where the coordinate system is chosen such that x-axis coincides with the (horizontal) direction of crack propagation. The shape of the fracture in the yz-plane is assumed to be elliptical, with the axis in vertical direction fixed at the fracture height h_f, and the axis in the horizontal direction equal to the fracture aperture, $w(x,t)$, which is defined on the one-dimensional time-dependent domain $\Omega(t) = [0, l(t)]$. The evolution in time of the fracture tip position, $l(t)$, and fracture aperture, $w(x,t)$, is driven by injection (at $x = 0$ with flow rate i) of an incompressible Newtonian fluid with dynamic viscosity μ. The considered model includes fluid loss effects, governed by the leakoff coefficient c_l, and fracture volume changes [4]. Plane strain behavior

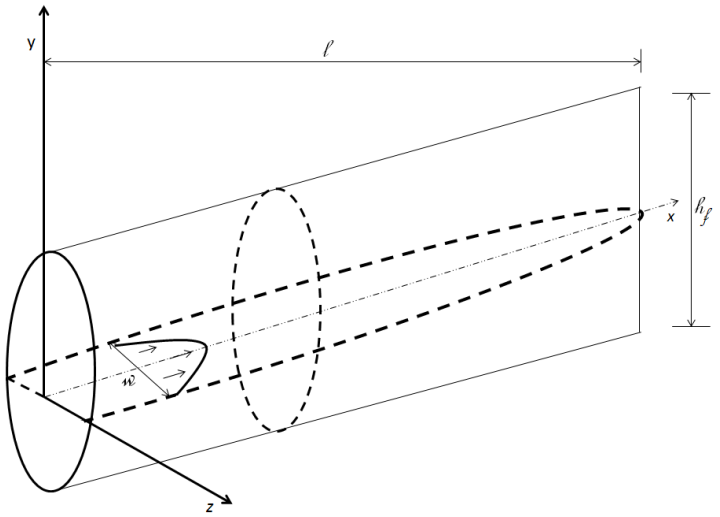

Figure 1: Schematic diagram of PKN fracture

in the vertical direction is assumed with plane strain modulus $E' = E/(1-\nu^2)$, where E and ν denote the Young's modulus and Poisson's ratio of the rock formation, respectively.

The PKN model is based on the conservation of mass of the fracturing fluid,

$$-\frac{\partial q}{\partial x} = C_L + \frac{\partial A_c}{\partial t}, \tag{1}$$

where $q(x,t)$ is the volume rate of flow through the fracture cross-section, C_L is the rate of fluid loss per unit length of the fracture, and $A_c = \frac{1}{4}\pi h_f w$ is the cross-sectionional area of the fracture. The fracture is assumed to be in an ellipitical shape [1]. And for the laminar flow of a Newtonian (fracturing) fluid, the flow rate is related to the pressure gradient by

$$\frac{\partial p}{\partial x} = \frac{64\mu q}{\pi w^3 h_f} \tag{2}$$

Under the plane strain assumption the fracture aperture can be related to the pressure by

$$p = \frac{E'}{2h_f} w \tag{3}$$

The fluid leakoff is governed by the empirical Carter model [10],

$$C_L = \frac{2h_f c_l}{\sqrt{t-\tau}} \tag{4}$$

where c_l is the leakoff coefficient and τ is the arrival time of the fracture tip at location x, *i.e.* $\tau(x) = l^{-1}(x)$. Substituting of equation (2), (3) and (4) in the balance equation (1) then yields the nonlinear partial differential equation

$$\frac{\pi E\prime}{4 \times 128\mu}\left(\frac{\partial^2 w^4}{\partial x^2}\right) = \frac{2h_f c_l}{\sqrt{t-\tau}} + \frac{\pi h_f}{4}\left(\frac{\partial w}{\partial t}\right) \tag{5}$$

subject to the following intitial and boundary conditions:

- Initial condition:
$$w(x,0) = q(x,0) = 0 \tag{6}$$

- The inlet condition – The fluid flow rate i at well-bore ($x = 0$) is constant in time and can, in view of (2) and (3), be expressed as
$$\frac{\partial w^4}{\partial x}(0,t) = -\frac{512\mu}{\pi E\prime} i. \tag{7}$$

- Tip condition – The conditions at the crack tip at $x = l(t)$ is
$$w(l(t),t) = 0. \tag{8}$$

The evolution of the domain $\Omega(t) = [x, l(t)]$ follows from [5]

$$\frac{\pi E\prime}{512\mu}\frac{\partial w^4}{\partial x} + \frac{\pi}{4}u_f h_f w + 2u_f h_f S_p = 0 \quad \text{at} \quad x = l, \tag{9}$$

where the tip propagation velocity, u_f, is the growth rate of the fracture length, i.e. $u_f = \dot{l}$. This equation conveys that the flow rate at the tip equals the sum of volume growth rate at the tip plus the rate of the spurt due to creating new surface. After rearrangement the tip velocity can be written as:

$$u_f = -\frac{\pi E\prime w^3}{32\mu h_f(\pi w + 8S_p)}\frac{\partial w}{\partial x}. \tag{10}$$

In our analysis we consider the special case formulated by Nordgren [4] fow which there are no spurt losses ($S_p = 0$) and the net pressure is zero at the tip (hence the width at the moving fluid front is zero).

We note that the nonlinearity of Equation (9) results in a weak singularity of the fracture aperture at the tip. It is important to note, however, that although the derivative $\frac{\partial w}{\partial x}$ is infinite, the tip velocity is finite by virtue of the fact that w itself goes to zero at the tip. From the perspective of numerical approximation it is essential to appropriately capture this tip singularity, as it governs the evolution of the fracture front. In the next Section 3 we discuss how we employ the eXtended Finite Element Method to adequately capture this singular behavior.

3 NUMERICAL APPROXIMATE METHOD

3.1 XFEM Discretization

Since the introduction of XFEM by Belytschko and Black, it has been employed in various settings to model fracture and propagation of cracks. XFEM can help to overcome imposed challenges and simplify the problems posed by traditional finite elements [7] in material modeling. In our present PKN model, the idea behind using XFEM is to enrich the usual finite element spaces with additional degrees of freedom, which incorporate the physics of the tip behaviour explained in Section 2. To include the singularity at the tip, we define a special enrichment function. The approximation of the fracture width w^h is given by

$$w^h = \sum_{i=1}^{n} N_i(x) w_i + \psi(x)\hat{w} \tag{11}$$

where the first part of the right hand side are the standard FEM shape functions with w_i are the nodal degrees of freedom and the second part represents the enrichment function, most often

based on asymptotic solutions. In case of the PKN model, the asymptotic expansion for crack opening is given by [12]

$$w(t,x) \approx w_0(t)(1-x)^{1/3} \tag{12}$$

The enrichment function used in our case is of the form $\psi = \hat{a}(l-x)^{1/3}$, where l is the fracture length and $\hat{a}$ is a constant. This special function is chosen because it satisfies the properties at the tip. The function becomes zero at the tip, $x = l$ and its derivative goes to minus infinity at $x = l$. When the spurt losses are zero $S_p = 0$, the propagation velocity becomes

$$u_f = -\frac{E\prime}{96\mu h_f}\left(\frac{\partial w^3}{\partial x}\right) \tag{13}$$

Thus, the derivative of the function $\psi^3(x)$ is a finite value. To compute an approximate solution to the strong form of the equations discussed in Section 2, the weak form of the problem with a test function v is given by

$$\int_0^L -\frac{\partial q}{\partial x} v dx = \int_0^L \frac{2h_f c_l}{\sqrt{t-\tau}} v dx + \int_0^L \frac{\pi h_f}{4}\left(\frac{\partial w_0}{\partial t}\right) v dx \qquad \forall v \tag{14}$$

Integrating by parts, results in the weak formulation:

$$iv(0) - L(w,v) = M(w,v)\frac{\partial w}{\partial t} + K(w,v)w \tag{15}$$

where $i\ (= q(0))$ is the inflow rate.

$$\begin{cases} K(w,v) = \int_0^L \frac{\pi w^3 h_f}{128\mu}\left(\frac{\partial w}{\partial x}\right)\left(\frac{\partial v}{\partial x}\right) dx \\ \\ M(w,v) = \frac{\pi h_f}{4}\int_0^L wv dx \\ \\ L(w,v) = \int_0^L \frac{2h_f c_l}{\sqrt{t-\tau}} v dx \end{cases} . \tag{16}$$

Note that the function $\tau(x)$ in the leakoff term is interpolated at the corresponding nodes of the mesh at time t for each step. The weak form (14) is discretized using the XFEM discretization (11). This leads to the non-linear system of equations:

$$iv(0) - L(w^h,v^h) = M(w^h,v^h)\frac{\partial w^h}{\partial t} + K(w^h,v^h)w^h \qquad \forall v^h \tag{17}$$

To solve this system of equations, we either use Picard or Newton iterations. For the sake of simplicity, we restrict our discussion to Picard iterations in the next section.

3.2 The incremental-iterative solution procedure

```
# Parameters
Input  : μ, i, h, E', DX, DT,nsteps
# Fracture geometry along with the pressure
Output : (w^1, l^1, p^1),(w^2, l^2, p^2)...(w^nstep, l^nstep, p^nstep)

# (1)Initialization
l^0, w^0

# Time loop starts
for k in range(nsteps):
    # (2)Propogation velocity and fracture length at current time
    u^tip
    l^k = l^{k-1} + u^tip * DT
    # (3) Define new domain, mesh
    domain,   nodes(1, 2, ...j, j + 1, ..)
    funcsp = FEMfuncsp + XFEMfuncsp
    # (4) Interpolate τ, w_j^{k-1} for every point on current mesh
    τ(x) = (l^k)^(-1)
    τ_j^k = Intepolate(τ(x))
    w_j^old = Interpolate(w^{k-1}(x))
    # solve for the width at the current step
    p^k, w^k = nonlinearsolver(w^old, points, geometry)
end

# To solve the resulting non linear equations
def nonlinearsolver(w^old, points, geometry):
    # Define solver parameters, relaxation factor for picard as α
    tol, maxiter, α
    while tol < toliter   and   iter < maxiter:
        iter  +=  1
        n = iter # n subscript denote the values at current iteration
        Kfunc , Mfunc, Lfunc                                  # see equation (15)
        f                                                      # inflow condition
        (w_j)_n = (Kfunc * DT + M).solve(f * DT − L * DT + (M.(w_j^old)))
        # Picard Iteration
        (w_j^k)_n = (w_j^k)_{n−1} + α((w_j^k)_n − (w_j^k)_{n−1})
        # tolerance of iteration
        toliter = f * DT − L * DT + (M.(wold)) − (K * DT + M).(w_n^k)
    end
    p^k = E' w^k/2h
    return p^k, w^k
end
```

Algorithm 1: Psuedo code of XFEM PKN model

The incremental-iterative solution procedure with which we compute the solution to the model presented above is described in Algorithm 1. With this algorithm it has to be noted that:

1. To avoid degeneracy as $t \to 0$, an initial approximation of l^0 and w^0 is considered. For instance, we consider a wedge shaped profile $w^0 = ww(1 - \frac{x}{l^0})$, where ww can be a very

small number.

2. With this initial approximation, we advance to next time steps (k). We compute tip velocity, u^k using equation (13).
3. With the new fracture length (l^k), we define the new domain, nodes and the basis functions as explained in equation (11).
4. We need to compute the values of τ_j, w_j^{k-1} (j representing node number). For this, we interpolate the function $\tau(x) = l^{-1}(x)$ to each node, τ_j. By projecting w^{k-1}, the width from the previous time step, onto the current mesh, we obtain w_i^{k-1}
5. The new w_j^k, p_j^k obtained by solving the nonlinear system of equations (17).

4 NUMERICAL SIMULATIONS

In this section we present the results obtained based on the XFEM formulation outlined in the previous section. We investigate the results using the data used in the comparative study by Warpinski *et al.* [8]. We study mesh convergence of the method. In Section 4.2, we present the sensitivity analysis for the various input parameters of the model.

4.1 Benchmark Result

The input data for our benchmark simulation is from [8] and all parameters are given in Table 1. The Figure 2(a), shows the width profile of the crack at different time steps. It can be observed from the width profile that the crack is widened after every time step. We validate the results with the test cases in [8] and observe that the results to be in good agreement.

c_l	$9.84 * 10^{-6}$ m/$s^{1/2}$
S_p	0 m
h_f	51.8 m
E'	6.13 x 10^{10} Pa
μ	0.2 Pa.s
i	0.0662 m^3/s

Table 1: Input data

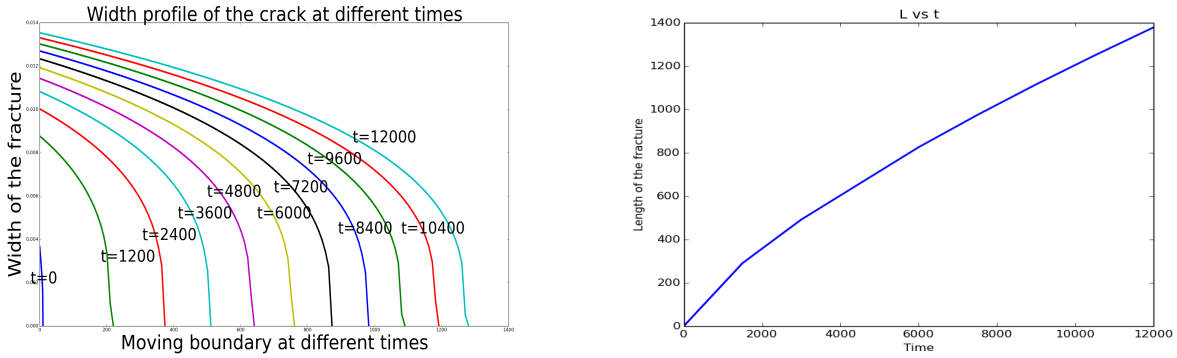

Figure 2: (a) Moving boundary at different times (b) Length of the fracture vs time

Studying mesh independence is important to assess the convergence of the method and to know the mesh size to obtain accurate results. We present the discretization aspects for both space and time steps in Table 2. We perform the simulations for time $T = 100$ seconds. These results are taken into consideration to perform sensitivity studies. Table 2 shows the length and maximum width of the fracture obtained after 100 seconds for corresponding space and time step. We take into consideration the Courant-Friedrichs-Levy condition (in our case, $\frac{u^{tip}\Delta t}{\Delta x}$) to set the limit for Δt. In order to keep the discretization error low, we take $\Delta x \leq \Delta t$. We therefore have, $0.1\Delta x \leq 0.1\Delta t \leq \Delta x$ in the Table 2. We compute the relative error for the length taking the mesh independent value as reference.

Time step (Δt)	Space step (Δx)	Fracture length (m)	Relative error for the length (%)	Maximum width (m)
0.5	0.4	32.805	3.61	0.0054
0.5	0.2	33.151	2.59	0.0054
0.5	0.1	33.264	2.26	0.0054
0.25	0.2	33.303	2.14	0.0054
0.25	0.1	33.626	1.20	0.0054
0.25	0.05	33.712	0.95	0.0054
0.125	0.05	33.034	0.00	0.0054
0.125	0.025	34.034	0.00	0.0054
0.125	0.0125	34.034	0.00	0.0054

Table 2: Step size dependence

It can be seen that after $\Delta x = 0.05$ and $\Delta t = 0.125$, the results become mesh independent for the length. For the meshes smaller than this the relative error is less than 0.001%. So we consider the step size $\Delta x = 0.05$ and $\Delta t = 0.125$ for the simulations in the next Section 4.2. In case of the width, we observe a change in the value between different step size is less than 10^{-3}. Note that these results are obtained using an adaptive mesh refinement startegy which refines the mesh as we get closer to the tip. These convergence results may vary on a different mesh.

4.2 Sensitivity analysis

The idea behind this section is to find the potentially important factors that influence a model. This is to identify the input factors that drive most of the variation in the output [9]. We choose independent input factors and perform numerical experiments to identify the impact on the output parameters. This screening exercise is often the first step to apply uncertainty quantification techniques on a model. It is to be noted that this method provides the qualitative sensitivity measure of the input factors, but does not quantify the importance of the factor on the output. So, in this section, the sensitivity of the process with respect to the properties of the fluid and the rock to the fracture geometry and fracturing pressure is analyzed for the PKN model with the formulation discussed in the previous section 3. The effects of fluid viscosity, Young's modulus of the rock, and the fluid leak-off coefficient on fracture geometry are studied. We do not consider the effect on the pressure in this case, as the width of the fracture and pressure are linearly related (3).

4.2.1 Viscosity of the fluid

For the numerical experiments, we consider the variation of the viscosity in the range of 0.05 Pa.s to 5 Pa.s and the values of the other parameters are the same as in Table 1. Figure 3 (a) shows that crack width increases with the increase in the fracturing fluid viscosity and Figure 3 (b) shows that the fracture length decreases with the increase in fluid viscosity. We can see from Figure 3 (c) that with a higher viscous fluid, a wider and shorter fracture is produced when compared to a lower viscous fluid which produces narrower and longer fractures.

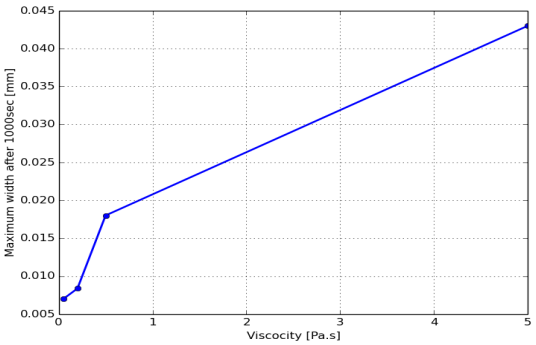

(a) Fracture maximum width changes with different fluid viscosities

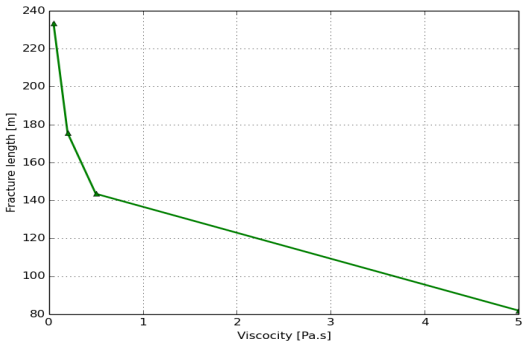

(b) Fracture length changes with different fluid viscosities

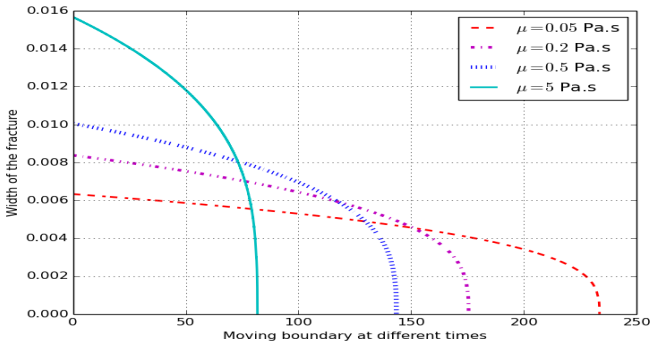

(c) Fracture geometry changes with different fluid viscosities

Figure 3: Effects of viscosity on the fracturing geometry

4.2.2 Plane strain modulus

We now consider the effect of plane strain modulus on the fracture geometry, while keeping the fluid and operation conditions unchanged. Inputting the plane strain modulus with values between 10^3 MPa and 10^4 MPa and running these cases, we get the following results. Figure 4 (a), (b), (c) express that a shorter and wider fracture will be generated when the formation is soft with a low plane strain modulus, while a longer and narrower fracture will be produced when the formation is hard with a high plane strain modulus, using the same fracturing fluid and operation conditions. When interpolated to pressure, the results indicate that higher fracturing pressure is required to fracture harder reservoirs which is inline with the experimental results [8].

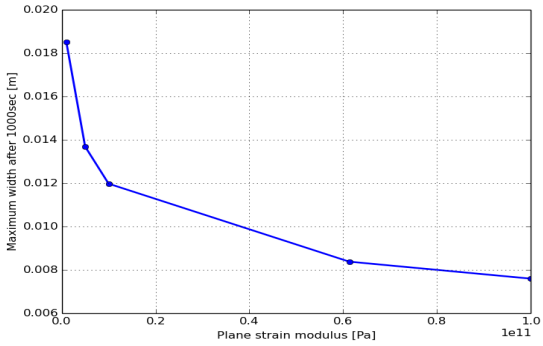

(a) Fracture maximum width changes with different plane strain moduli

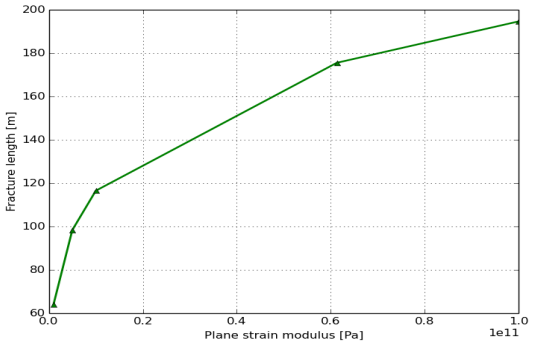

(b) Fracture length changes with different plane strain moduli

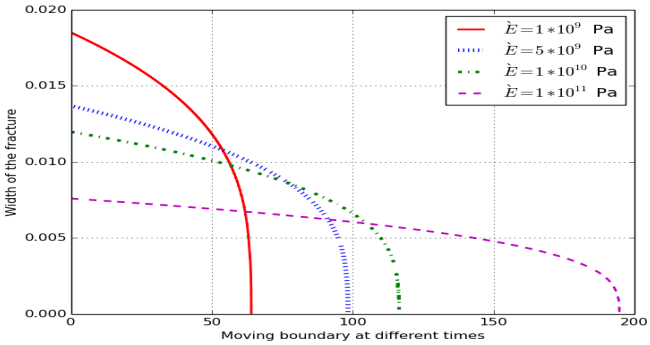

(c) Fracture geometry changes with different plane strain moduli

Figure 4: Effects of plane strain modulus on the fracturing geometry

4.2.3 Leakoff coefficient

The leakoff coefficient is a parameter which is dependent on both fluid and formation properties. By keeping the other parameters unchanged, the effect of the leakoff coefficient is studied. Figures 5 (a), (b), (c) show that the fracture length and width decrease when the leakoff coefficient is decreased.The leakoff coefficient has a different effect when compared to fluid viscosity and the plane strain modulus. When the leakoff coefficient is higher, smaller and narrower fractures are obtained.

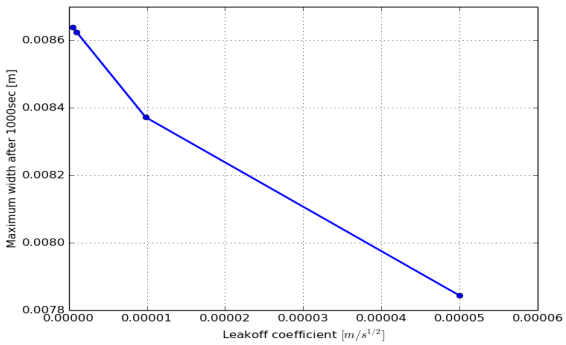

(a) Fracture maximum width changes with different leakoff coefficients

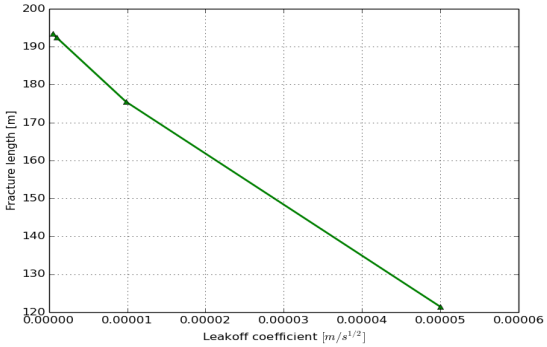

(b) Fracture length changes with different leakoff coefficients

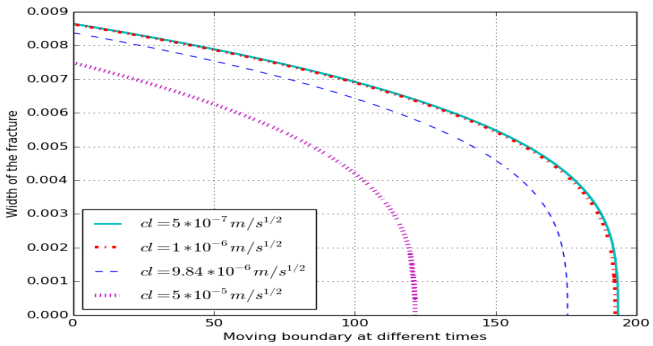

(c) Fracture geometry changes with different leakoff coefficients

Figure 5: Effects of leakoff coefficient on the fracturing geometry

5 CONCLUSIONS AND FUTURE WORK

In the PKN model we considered the three independent input parameters of the model and varied these independently to observe the change in the fracture geometry. The results obtained by the parameter change can be summarized in Figure 6. The parameter change is taken from the base values of Table 1.

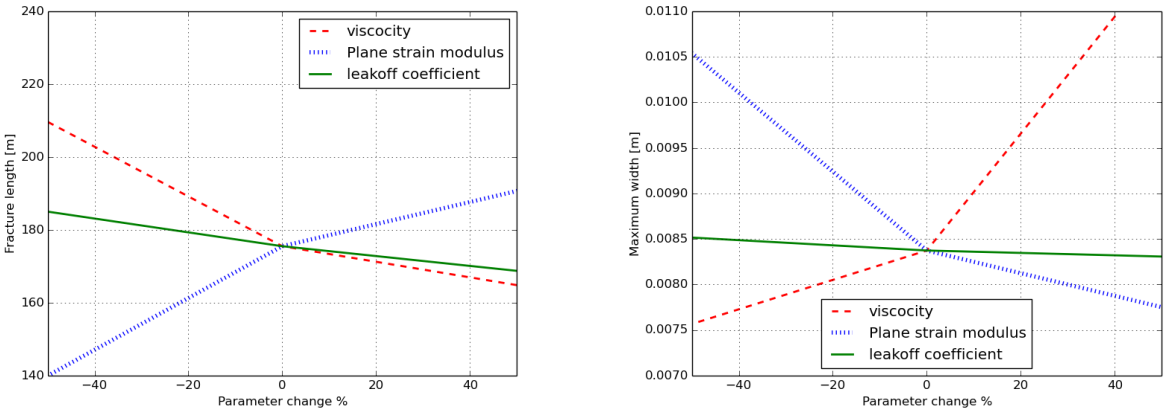

(a) length vs parameter change

(b) width vs parameter change

Figure 6: Effects of multiple parameters on fracture geometry

The following conclusions are drawn from the numerical experiments of the sensitivity analysis:

- **Fracture length**: Both viscosity and the leakoff coefficient have the same effect on fracture length when they are changed, yet we notice that fracture length is more sensitive to the viscosity than to the leakoff coefficient. The plane strain modulus has a different effect, as the fracture length increases with an increase of its value.
- **Fracture width**: Width decreases with an increase of leakoff coefficient or plane strain modulus. However, fracture width is less sensitive to the leakoff coefficient than the plane strain modulus. Although the effect of viscosity on the width is opposite when compared to the other parameters, it can be seen that the width is more sensitive to it.

Note that similar conclusions can be drawn from analytical solution or from dimensional analysis. However, our idea is to apply stochastic methods in the framework of hydraulic fracturing which requires high accuracy. To accomplish this, we applied XFEM to the PKN model.

The sensitivity analysis presented herein serves as the basis for the development of an uncertainty quantification framework based on Bayesian inference.

REFERENCES

[1] T.K. Perkins, L.R. Kern, Widths of hydraulic fractures, *Society of Petroleum Engineers*, **13**(9), 937-949, 1961.

[2] P. Valko, M.J. Economides, *Hydraulic fracturing,* 2^{nd} *Edition*. Wiley, 1995.

[3] Y. Kovalyshen, E. Detournay, A Reexamination of the Classical PKN Model of Hydraulic Fracture. *Transport in Porous Media*, **81**, 317-339, 2010.

[4] R. Nordgren, Propagation of Vertical Hydraulic Fractures. *Society of Petroleum Engineers*, **12**(4), 306-314, 1972.

[5] L.F. Kemp, Study of Nordgren's equation of Hydraulic Fracturing. *SPE Production Engineering*, **5**(3), 311-314, 1990.

[6] E. Detournay, A.H.D. Cheng, J.D. McLennan, A Poroelastic PKN Hydraulic Fracture Model Based on an Explicit Moving Mesh Algorithm. *ASME. J. Energy Resour. Technol.*, **112**(4),224-230, 1990.

[7] T. Belytschko, R. Gracie, G. Ventura, A review of extended/generalized finite element methods for material modeling. *Modelling and Simulation in Materials Science and Engineering*, **17**(4), 043001, 2009.

[8] N.R. Warpinki, Z.A. Moschovidis, C.D. Parker and Abou-Sayed, IS.: Comparison Study of Hydraulic Fracturing models: Test Case - GRI-Staged Experiment No. 3. *SPE Production Engineering and Facilities*, **9**(1), 7-16, 1994.

[9] A. Saltelli, S. Tarantola, F. Campolongo, M. Ratto, *Sensitivity Analysis in Practice: A Guide to Assessing Scientific Models*. Wiley, 2004.

[10] G.C. Howard, C.R. Fast, Optimum Fluid Characteristics from Fracture Extension, *API Drilling and Production Practice*, **24**, 261-270, 1957.

[11] E. Detournay, Mechanics of Hydraulic Fractures. *Annual Review of Fluid Mechanics*, **48**, 311-339, 2016.

[12] M. Economides, K. Nolte, *Reservoir Stimulation,* 3^{rd} *Edition*. Wiley, 2000.